

HOW TO COPE WITH UNCERTAINTIES IN BOUNDARY CONDITIONS AND COUPLINGS OF SUBSTRUCTURES

N. Wagner, R. Helfrich
(INTES GmbH, Germany)

Abstract

It is well known that results of finite element simulations are subject to considerable uncertainty associated with the operating conditions. Substantial differences between experimental and CAE results persists even when material parameters such as mass and stiffness are updated in order to match experimentally determined eigenfrequencies. It turns out that the couplings of substructures are afflicted with uncertainties. In the beginning the different parts of a finite element model are usually tied together. However, the position and exact size of the corresponding glued areas under operating conditions are not known a priori. In this study, a two-step approach is established to cope with these uncertainties. The first step is a contact analysis which considers the different loads of the mounting situation and final operating conditions. Based on the results from the previous contact analysis, active contacts are replaced by linear multipoint constraints. Moreover, a different treatment of normal and tangential directions of frictional contacts is available in order to mimic a realistic behaviour. A further kind of fuzziness can be introduced here by using the current contact pressure. Once the actual contact pressure exceeds a certain threshold a multipoint constraint is introduced. On that basis, a modal analysis is performed to compute the eigenfrequencies of the structure. Additional effects such as pretension can be taken into account by using the geometric stiffness matrix. An example for a joint structure is used to demonstrate the procedure using the commercial finite element package PERMAS. A comparison between the eigenfrequencies of a classically tied assembly and the new approach illustrates the paramount importance of an appropriate modelling of interfaces in jointed structures.

1. Overview

Different blade root types, such as hammer type or T-type, fir tree, threaded, dove tail, Straddle and Laval are used in the industry [12]. All these concepts ensure that the blades are tightly fitted on the disc. A removal of the blades for replacement, repair or refurbishment is assured. Nowadays the most common attachment type is a fir tree.

Centrifugal forces lead to a load on the blades that can be extremely high during operation. Blade failures in gas turbine engines often lead to loss of all downstream stages and can have a dramatic effect on the availability of the turbine engines (Hou [3]). Therefore failure analysis of blades is investigated in many publications.

Meguid [8] conducted a three-dimensional FE-analysis of the fir-tree region on aero-engine turbine disc assemblies. Song [13] investigated the turbine blade fir-tree root design optimization. Fatigue life is discussed by Hou [4] and Witek [14]. Creep in turbine disc fir-tree is considered by Maharaj [6]. Aschenbruck et. al. [1] investigated the fir-tree clamp by an experimental setup and compared the results with a finite element model. They pointed out, that the boundary conditions of the model need to be adjusted to match the eigenfrequencies of the experimental results. The dynamical behaviour depends also on the type of root, and even more on the tightness of the contact between the disc and the blade. The tightness of the contact is mainly influenced by applied loads, e.g. temperature, centrifugal forces. Hence the contact can be weak or with some clearance and can develop as rigid contact at rated speed. Temperature effects are neglected in the current study since the centrifugal loads are usually the most critical loads acting on a turbine disc. However, the influence of high temperatures can be found in Madhavan [5] and Witek [14].

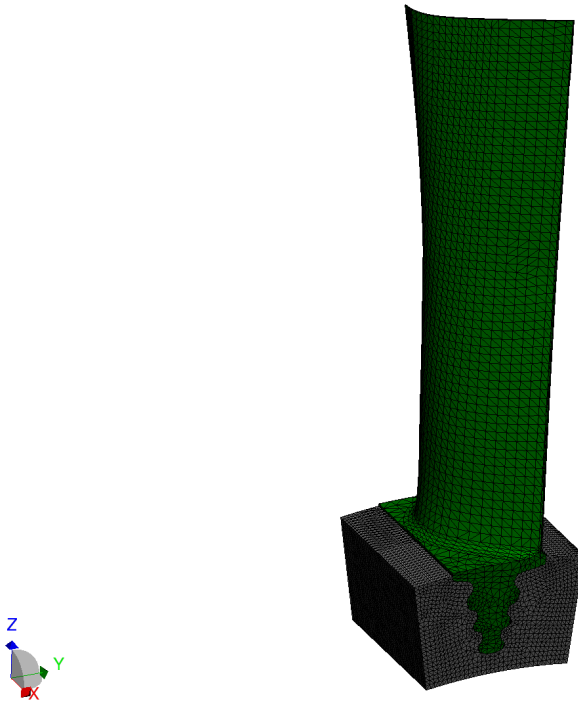
To examine the dynamic behaviour of the blade, a pre-stressed modal analysis was performed for the disc and blade assembly. Only a single sector is considered here. PERMAS [15] specific commands are highlighted by a preceding dollar sign and capital letters in the subsequent sections.

2. Numerical example

The finite element model of the blade-disc assembly is depicted in Fig. 1. The material properties of the blade and disc are listed in Table 1.

Table 1: Material parameters of the blade-disc assembly

Young's modulus E [GPa]	70.
Poisson's ratio ν	0.33
Density ρ [kg/m ³]	2780.

*Figure 1: Finite element model of a blade-disc assembly*

It contains 181622 second-order tetrahedral elements. The disc sector is fully clamped at the inner part. A surface-to-node contact is introduced at the interface of adjacent surfaces of the disc and blade. Possible rigid body modes of the blade are detected by the so-called RBM-assistant in VisPER (Visual PERMAS) [16]. As soon as the definition of contacts is complete, the RBM assistant may be used to define an elastic support of the contact bodies. For this purpose,

disconnected mesh regions are detected on the first page of the wizard. Multipoint constraints and possible pretension definitions are taken into account as connections. The second page of the RBM assistant is dedicated to detect further candidates for possible rigid body motions. The detection starts from each contact definition to find the affected parts. At this time multipoint constraints will be ignored since they have an impact only some degrees of freedom and allow for further rigid body motions. Already processed parts of the previous step will be skipped.

Finally, a static analysis with a series of increasing centrifugal force levels is applied to mimic the tightness variation of the contact. Centrifugal forces generated during service by rotation of the disc were simulated by applying an angular velocity to all elements in the model. A threshold value for the minimal contact pressure is used to adapt the size active contact areas. The maximum contact pressure is located on the upper side of the lowest fir-tree (see Fig. 2).

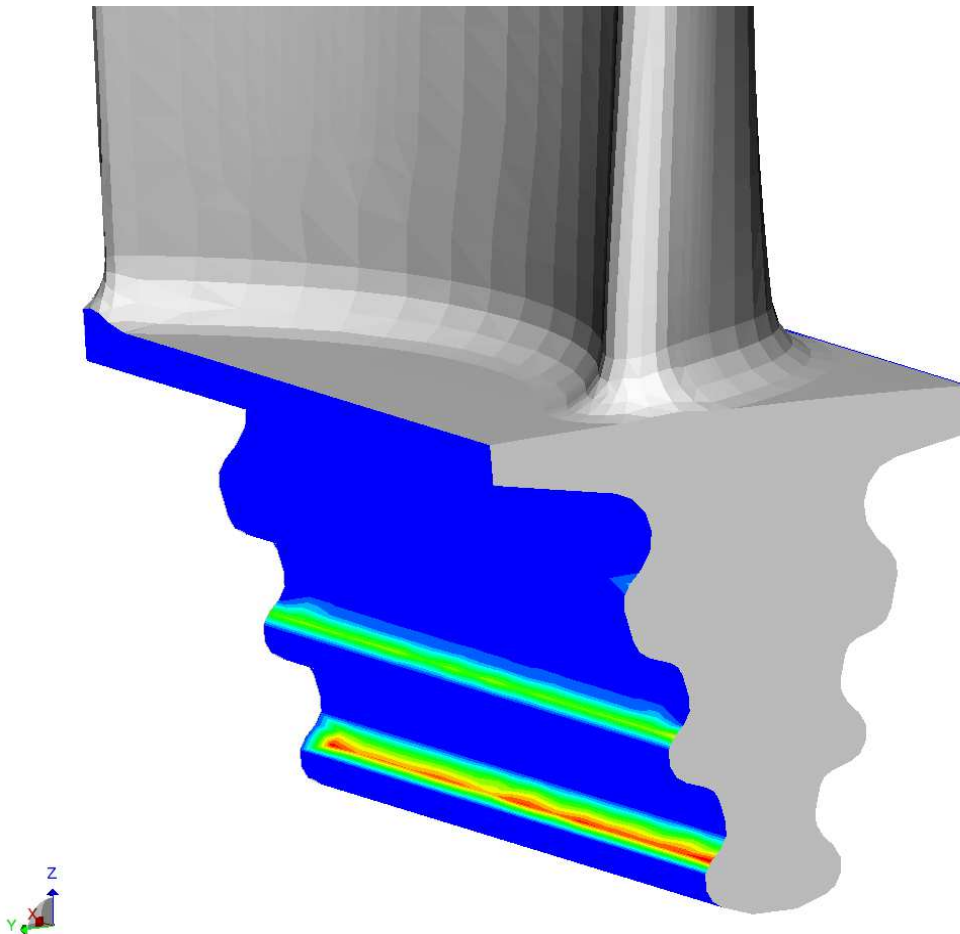


Figure 2: Contact pressure distribution

The remaining zones of the fir-tree are not as highly loaded as the serration region Fig. 3.

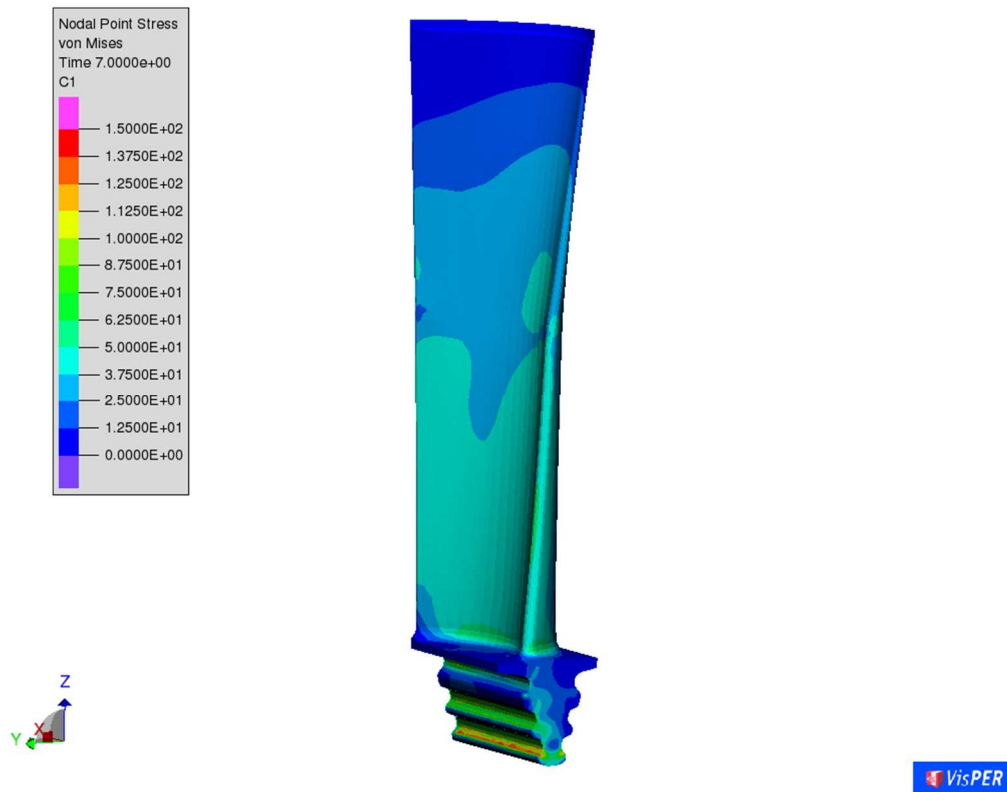


Figure 3: Nodal point stress distribution due to centrifugal loading

Afterwards all active contacts above the user-specified threshold value are automatically replaced by general multipoint constraints using the \$CONTLOCK statement in PERMAS. These internally generated multipoint constraints can be visualized in VisPER. Each contact definition and normal and tangential directions (in case of frictional contacts) can be handled separately.

The last step is an eigenvalue analysis of the linearized problem. The areas of active contact zones increase with the rotational speed. The upper limit is given by a fully tied contact between the disc and the blade. This effect is illustrated in Fig. 4 for the first ten eigenfrequencies of the assembly. The additional geometric stiffness is neglected in order to compare the influence of the contact linearization only. The percentage changes in eigenfrequencies is higher for lower

eigenmodes, e.g. 24 % for the first bending mode (f_1 in Fig. 5). The eigenfrequency change of the first torsional mode (f_3 in Fig. 6) is 1%. The number of general MPCs increases from 383 to 507.

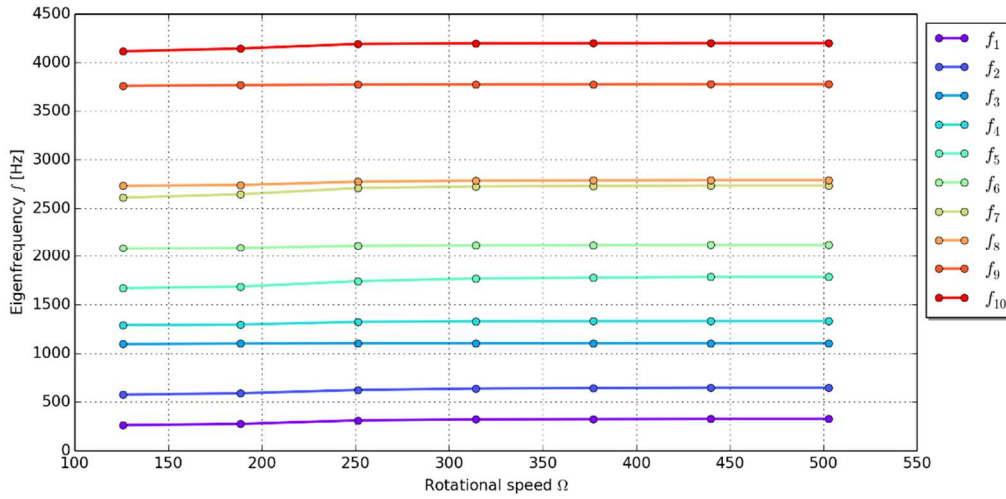


Figure 4: Spreading of natural eigenfrequencies

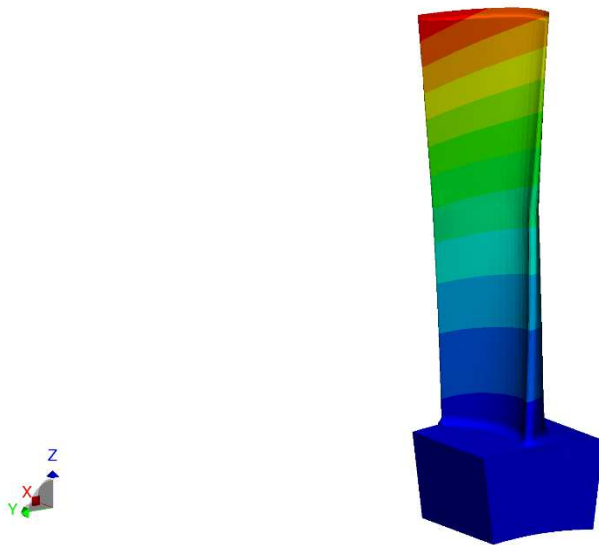


Figure 5: First bending mode $f_1 = 262.5$ [Hz]

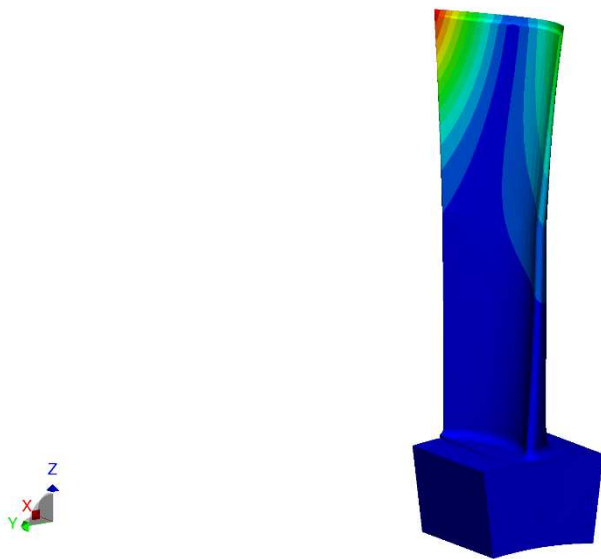


Figure 6: First torsional mode $f_3 = 1094.7$ [Hz]

3. Conclusions

A two-step procedure for the computation of eigenfrequencies of a single blade-disc assembly is presented. At the beginning a contact analysis is conducted. A linearization of the nonlinear contacts based on the results of the contact analysis is performed. Several aspects of the various possibilities in contact linearization are examined. A significant variability in natural frequencies is observed. This effect should be taken into account if results from an experimental modal analysis are compared with numerical simulations.

4. References

- [1] schenbruck, Jens; Meinzer, Christopher E.; Pohle, Linus; Panning-von Scheidt, Lars; Seume, Jörg R. (2013) Regeneration induced forced response in axial turbines, Proceedings of the ASME Turbo Expo, San Antonio, Texas, USA
- [2] Bachschmid, Nicolo; Pesatori, Emanuel; Bistolfi, Simone; Ferrante, Michele; Chatterton, Steven (2011) On impulsive vibration tests of shrouded blade rows. International Conference Surveillance 6, UTC
- [3] Hou, J.; Wicks, B. (2002), Root flexibility and untwist effects on vibration characteristics of a gas turbine blade, DSTO Platforms Sciences Laboratory, Australia

- [4] Hou, J.; Wicks, B.; Antoniou, Ross A. (2002) An investigation of fatigue failures of turbine blades in a gas turbine engine by mechanical analysis, *Engineering Failure Analysis*, Vol. 9, pp. 201-211.
- [5] Madhavan, S.; Jain, Rajeev; Sujatha C.; Sekhar, A.S. (2014) Vibration based damage detection of rotor blades in a gas turbine engine, Vol. 46, pp. 26—39.
- [6] Maharaj, Chris; Morris, Andy; Dear, John P. (2012), Modelling of creep in Inconel 706 turbine disc fir-tree, *Materials Science & Engineering A*, Vol. 558, pp. 412—421.
- [7] Maktouf, Wassim; Sai, Kacem (2015) An investigation of premature fatigue failures of gas turbine blade, *Engineering Failure Analysis*, Vol. 47, pp. 89—101.
- [8] Meguid, S.A.; Kanth, P.S.; Czekanski, A. (2000) Finite element analysis of fir-tree region turbine discs. *Finite Elements in Analysis and Design*, Vol. 35, pp. 305—317.
- [9] Naumann, Helmut G. (1982), Steam turbine blade design options: How to specify or upgrade. *Proceedings of the 11th Turbomachinery symposium*, Houston, Texas, USA, pp. 29—50.
- [10] Poursaedi, E.; Aieneravaie, M. (2008), Failure analysis of a second stage blade in a gas turbine engine, *Engineering Failure Analysis*, Vol. 15, pp. 1111—1129.
- [11] Poursaedi, E.; Mohammadi, M. R. (2008), Failure analysis of lock-pin in a gas turbine engine, *Engineering failure Analysis*, Vol. 15, pp. 847—855.
- [12] Raczynski, Adam (2010), *Gas turbine blade vibration – Influencing factors and their effects*. Lambert Academic Publishing.
- [13] Song, Wenbin; Keane, Andy; Rees, Janet; Bhaskar, Atul; Bagnall, Steven (2002), Turbine blade fir-tree root design optimisation using intelligent CAD and finite element analysis, *Computers and Structures*, Vol. 80, pp. 1853—1867.
- [14] Witek, Lucjan (2006), Failure analysis of turbine disc of an aero engine, *Engineering Failure Analysis*, Vol. 13, pp. 9—17.
- [15] PERMAS User's Reference Manual, INTES Publication No. 450
- [16] VisPER User Manual, INTES Publication No. 470.

[17] <http://www.intes.de>